Acta Crystallographica Section B
Structural Science
ISSN 0108-7681

Structures of stable and metastable $Ge_2Bi_2Te_5$, an intermetallic compound in a GeTe–Bi_2Te_3 pseudobinary system

Toshiyuki Matsunaga,[a,b]* Rie Kojima,[c] Noboru Yamada,[b,c] Kouichi Kifune,[d] Yoshiki Kubota[e] and Masaki Takata[b,f]

[a]Characterization Technology Group, Matsushita Technoresearch Inc., 3-1-1 Yagumo-Nakamachi, Moriguchi, Osaka 570-8501, Japan, [b]CREST, Japan Science and Technology Agency, 4-1-8 Honmachi, Kawaguchi, Saitama 332-0012, Japan, [c]AV Core Technology Development Center, Matsushita Electric Industrial Co. Ltd, 3-1-1 Yagumo-Nakamachi, Moriguchi, Osaka 570-8501, Japan, [d]Faculty of Liberal Arts and Sciences, Osaka Prefecture University, 2-1 Daisen-cho, Sakai, Osaka 590-0035, Japan, [e]Graduate School of Science, Osaka Prefecture University, 2-1 Daisen-cho, Sakai, Osaka 590-0035, Japan, and [f]Japan Synchrotron Radiation Research Institute (JASRI), 1-1-1 Kouto, Sayo-cho, Sayo-gun, Hyogo 679-5198, Japan

Correspondence e-mail: matsunaga.toshiyuki@jp.panasonic.com

Received 19 July 2006
Accepted 8 January 2007

$Ge_2Bi_2Te_5$ in the GeTe–Bi_2Te_3 pseudobinary system has two single-crystalline phases: a metastable phase with an NaCl-type structure and a stable phase with a nine-layer trigonal structure. In the metastable phase, the structure consists, in the hexagonal notation, of infinitely alternating stacks of Te and Ge/Bi layers at equal intervals along the *c* axis. On the other hand, in the stable phase those two layers are stacked alternately nine times to form an NaCl block. The blocks are then piled to construct a nine-layered trigonal structure with cubic close-packed stacking. Both ends of each block are covered with Te layers, contrary to the infinite alternation of Ge/Bi and Te layers in the structure of the metastable phase. The Ge/Bi layers in the metastable phase contain as much as 20 at. % vacancies; on the other hand, those in the stable phase are filled with atoms. These two crystalline phases in $Ge_2Bi_2Te_5$ have identical atomic configurations to the two corresponding phases found in $Ge_2Sb_2Te_5$.

1. Introduction

Today, the most widely used memory material for rewritable phase-change optical disks, such as digital versatile disk–random access memory (DVD–RAM), is a GeTe$(1-x)$–$Sb_2Te_3(x)$ pseudobinary compound. An optical disk records the changes in its optical characteristics during the phase transformation between the amorphous and crystalline phases of the material (Yamada *et al.*, 1991). These pseudobinary amorphous films are transformed into NaCl-type structures as a metastable phase by instantaneous laser annealing over a wide range of compositions, from GeTe (x = 0) to at least $GeSb_4Te_7$ (x = 2/3; Matsunaga *et al.*, 2006). However, in a thermal equilibrium state, it is known that this pseudobinary system has various intermetallic compounds represented by the chemical formula $(GeTe)_n(Sb_2Te_3)_m$ (Karpinsky *et al.*, 1998*b*). These compounds, which are called a homologous series, can be described as structures with cubic close-packing periodicity ($\cdots ABCABC\cdots$), where the stacking rules of the Ge, Sb and Te layers differ from each other. In this GeTe–Sb_2Te_3 pseudobinary system, it was found several years ago that the crystallization speed, namely the rewrite speed, can be improved when a proportion of Sb is replaced by Bi (Yusu *et al.*, 2002). The GeTe–Bi_2Te_3 pseudobinary compounds as well as the GeTe–Sb_2Te_3 compounds form another homologous series in a thermal equilibrium state (Shelimova *et al.*, 2004). We have already investigated the structure of the $Ge_2Sb_2Te_5$ stable phase, which is one of the GeTe–Sb_2Te_3 homologous series (Matsunaga *et al.*, 2004). However, for $Ge_2Bi_2Te_5$, neither its crystal structure nor even its existence has been clarified yet. In their X-ray study on the Ge–Bi–Te homologous-series compounds, Karpinsky *et al.* (1998*a*) found that

Table 1
Experimental details.

	Metastable		Stable	
	87 K	293 K	87 K	293 K
Crystal data				
Chemical formula	$Ge_{1.6}Bi_{1.6}Te_4$	$Ge_{1.6}Bi_{1.6}Te_4$	$Ge_2Bi_2Te_5$	$Ge_2Bi_2Te_5$
M_r	960.83	960.83	1201.04	1201.04
Cell setting, space group	Cubic, $Fm\bar{3}m$	Cubic, $Fm\bar{3}m$	Trigonal, $P\bar{3}m1$	Trigonal, $P\bar{3}m1$
Temperature (K)	87	293	87	293
a, b, c (Å)	6.0932 (5), 6.0932, 6.0932	6.1109 (9), 6.1109, 6.1109	4.28072 (12), 4.28072, 17.2651 (6)	4.30040 (13), 4.30040, 17.3659 (6)
α, β, γ (°)	90, 90, 90	90, 90, 90	90, 90, 120	90, 90, 120
V (Å^3)	226.22 (3)	228.20 (6)	273.99 (1)	278.13 (2)
Z	1	1	1	1
D_x (Mg m^{-3})	6.98	6.96	7.28	7.17
Radiation type	Synchrotron	Synchrotron	Synchrotron	Synchrotron
μ (mm^{-1})	11.52	11.51	12.03	11.85
Specimen form, colour	Cylinder, dark gray	Cylinder, dark gray	Cylinder, metallic dark gray	Cylinder, metallic dark gray
Specimen size (mm)	3.0 × 0.1	3.0 × 0.1	3.0 × 0.1	3.0 × 0.1
Specimen preparation cooling rate (K min^{-1})	0	0	0	0
Specimen preparation pressure (kPa)	0.0002	0.0002	0.0002	0.0002
Specimen preparation temperature (K)	300	300	300	300
Data collection				
Diffractometer	Debye–Scherrer camera	Debye–Scherrer camera	Debye–Scherrer camera	Debye–Scherrer camera
Data collection method	Specimen mounting: sealed quartz capillary tube; mode: transmission; scan method: fixed	Specimen mounting: sealed quartz capillary tube; mode: transmission; scan method: fixed	Specimen mounting: sealed quartz capillary tube; mode: transmission; scan method: fixed	Specimen mounting: sealed quartz capillary tube; mode: transmission; scan method: fixed
Absorption correction	None	None	None	None
2θ (°)	$2\theta_{min}$ = 5.0, $2\theta_{max}$ = 37.5, increment = 0.01	$2\theta_{min}$ = 5.0, $2\theta_{max}$ = 32.0, increment = 0.01	$2\theta_{min}$ = 1.0, $2\theta_{max}$ = 37.6, increment = 0.01	$2\theta_{min}$ = 1.0, $2\theta_{max}$ = 37.33, increment = 0.01
Refinement				
Refinement on	I_{net}	I_{net}	I_{net}	I_{net}
R factors and goodness of fit	R_p = 0.013, R_{wp} = 0.018, R_{exp} = 0.028, R_B = 0.005, S = 0.66	R_p = 0.015, R_{wp} = 0.024, R_{exp} = 0.038, R_B = 0.007, S = 0.62	R_p = 0.018, R_{wp} = 0.028, R_{exp} = 0.038, R_B = 0.016, S = 0.74	R_p = 0.021, R_{wp} = 0.035, R_{exp} = 0.021, R_B = 0.021, S = 1.73
Wavelength of incident radiation (Å)	0.42182	0.42182	0.42182	0.42206
Excluded region(s)	None	None	None	None
Profile function	Pseudo-Voigt	Pseudo-Voigt	Pseudo-Voigt	Pseudo-Voigt
No. of parameters	28	27	36	36
Weighting scheme	Based on measured s.u.'s	Based on measured s.u.'s	Based on measured s.u.'s	Based on measured s.u.'s
$(\Delta/\sigma)_{max}$	< 0.0001	< 0.0001	< 0.0001	< 0.0001
Preferred orientation correction	March–Dollase function, axis (511)	March–Dollase function, axis (100)	March–Dollase function, axis (103)	March–Dollase function, axis (001)

Computer programs used: *RIETAN* (Izumi & Ikeda, 2000).

$Ge_{1.5}Bi_{2.5}Te_5$ has a stable $Ge_2Sb_2Te_5$ nine-layered trigonal isostructure. They assumed that these two compounds, $Ge_{1.5}Bi_{2.5}Te_5$ and $Ge_2Bi_2Te_5$, have identical structures. In this work, we scrutinized the $Ge_2Bi_2Te_5$ crystal structures by an X-ray powder diffraction method using the facilities of the Japan Synchrotron Radiation Research Institute (SPring-8) to obtain clues to develop new optical phase-change materials with a better performance. Furthermore, this class of materials has considerable importance because the alloys in them are used for rewritable optical recording materials, and in the future will be applied to non-volatile electronic memories and thermoelectric energy conversion devices. Our structural investigation found that this compound has two crystalline phases, metastable and stable, as in the case of the $Ge_2Sb_2Te_5$ compound. An amorphous $Ge_2Bi_2Te_5$ film crystallizes through instantaneous annealing into a single metastable phase with an NaCl-type structure. In this structure the Cl site is completely occupied by Te atoms, whereas the Na site is randomly occupied by Ge and Bi atoms, and vacancies. On the other hand, the metastable face-centered cubic phase was transformed through sufficient annealing into a stable phase with a nine-layered trigonal structure. This is an isostructure of the $Ge_2Sb_2Te_5$ stable phase. In the structure of the $Ge_2Bi_2Te_5$ stable phase, Ge and Bi do not independently occupy their

Table 2
Refined structural parameters are shown for the $Ge_2Bi_2Te_5$ metastable (space group $Fm\bar{3}m$) and stable ($P\bar{3}m1$) phases at 87 K (space group $Fm\bar{3}m$).

	Site	*g*	*x*	*y*	*z*	*B* (Å^2)
Metastable phase						
Te	4(*a*)	1.0	0	0	0	1.51 (5)
$Ge_{0.5}Bi_{0.5}$	4(*b*)	0.781 (5)	1/2	1/2	1/2	2.50 (6)
Stable phase						
Te1	1:1(*a*)	1.0	0	0	0	0.15 (11)
Ge/Bi1	2:2(*d*)	0.638/0.362 (7)	2/3	1/3	0.1069 (3)	1.41 (8)
Te2	3:2(*d*)	1.0	1/3	2/3	0.2031 (2)	0.60 (8)
Ge/Bi2	4:2(*c*)	0.362/0.638	0	0	0.3263 (2)	1.32 (7)
Te3	5:2(*d*)	1.0	2/3	1/3	0.4212 (2)	0.83 (9)

respective sites or layers but randomly occupy both sites (layers), as in its metastable phase and both $Ge_2Sb_2Te_5$ crystalline phases.

2. Experimental

The diffraction measurement specimen was made using the following method. First, a thin film of $Ge_2Bi_2Te_5$, *ca* 3000 Å thick, was sputtered onto a glass disk with a 120 mm diameter. Inductively coupled plasma (ICP) atomic emission spectrometry confirmed that the composition of the specimen was close to $Ge_2Bi_2Te_5$. The film was amorphous just after its formation and was crystallized by laser irradiation into a metastable phase. The film was then powdered by scraping with a spatula and the powder was packed into a quartz capillary tube with an internal diameter of 0.1 mm. To insulate the powder against the atmosphere, the opening of the capillary was melted shut with an oxyacetylene flame.

A diffraction experiment was performed using the BL02B2 beamline at SPring-8 (Nishibori *et al.*, 2001). A precollimator mirror and a double-crystal monochromator were used to ensure that the incident beam utilized for the diffraction experiments was highly monochromatic and parallel. The energy of the incident beam was 29.391 keV (λ = 0.42182 Å). Intensity data were collected using a Debye–Scherrer camera with a 287 mm radius. An imaging plate with a pixel area of 100 μm^2 was used as the detector. Angular resolution was 0.02°. To improve the accuracy of the structural analyses, intensity data in increments of 0.01° were obtained by reading the imaging plate for a pixel area of 50 μm^2. The energy of the synchrotron radiation used was confirmed by recording the diffraction intensity of CeO_2 (*a* = 5.4111 Å) powder as a reference specimen at room temperature under the same conditions. High- and low-temperature experiments were performed while nitrogen gas was blown onto the capillary tube and set at specified temperatures. The measurement temperatures were controlled as 87 → 143 → 191 → 240 → 293 → 380 → 437 → ... (about 50 K intervals) ... → 930 → 984 K. These temperatures were calibrated in advance with a thermocouple placed in an identical position to the specimen holder (capillary tube). The mean heating rate from measurement to measurement was 10 K min^{-1}. After these temperature measurements, we annealed another metastable crystalline powder specimen at 851 K for 5 min to transform it into the stable phase. Using this specimen, another series of temperature measurements was conducted at 851, 293 and 87 K. The crystal structures were refined using the Rietveld method (Rietveld, 1969). Here, the *RIETAN* program was used (Izumi & Ikeda, 2000). Full experimental details are given in Table 1.

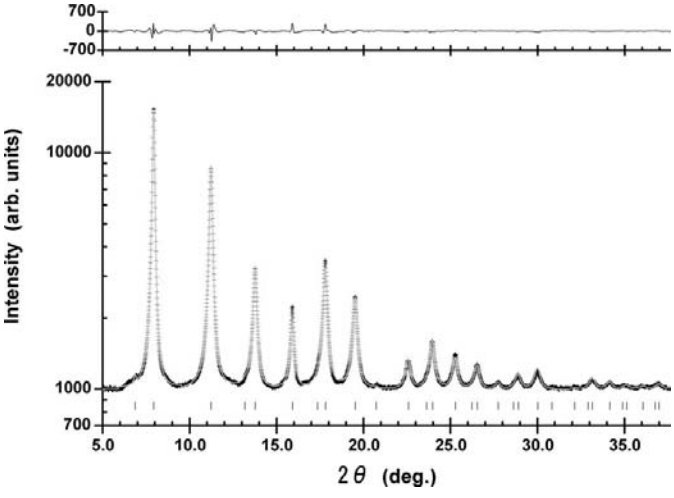

Figure 1
Observed (+) and calculated (gray line) X-ray diffraction profiles are shown for the $Ge_2Bi_2Te_5$ metastable phase at 87 K. Profiles are shown in a logarithmic scale, and under them reflection markers are indicated by vertical spikes. A difference curve (observed − calculated) appears at the top in a linear scale.

3. Results

3.1. Crystal structure of metastable phase

The structural analysis results of the $Ge_2Bi_2Te_5$ metastable phase are shown in Table 2 and Fig. 1. This phase has an NaCl-

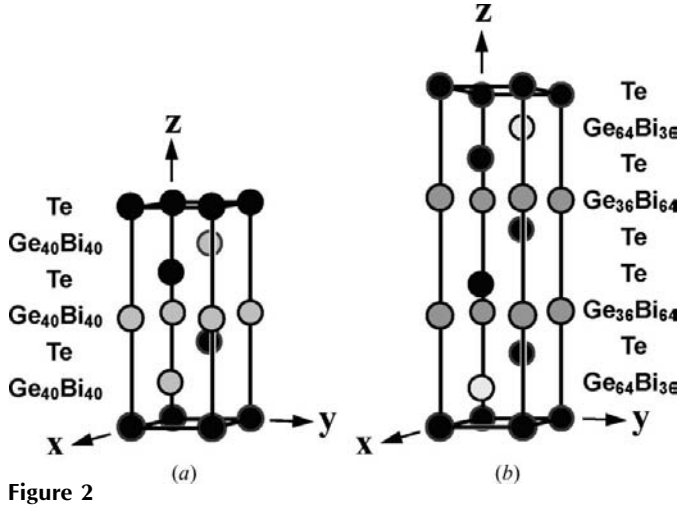

Figure 2
Crystal structures of (*a*) metastable and (*b*) stable $Ge_2Bi_2Te_5$ are shown schematically in perspective. The metastable cubic structure is depicted in a hexagonal unit cell. Black circles show the atomic positions for Te; gray circles show those for Ge or Bi.

Table 3
Temperature dependences of structural parameters for the $Ge_2Bi_2Te_5$ powdered specimen.

Standard uncertainties are shown in parentheses. The bottom two rows show data obtained using another specimen annealed at 851 K.

Atom	Ge/Bi1	Ge/Bi1	Te2	Ge/Bi2	Te3
site	2:2(*d*)	2:2(*d*)	3:2(*d*)	4:2(*c*)	5:2(*d*)
parameter	g_{Ge}/g_{Bi}	*z*	*z*	*z*	*z*
660 K	0.65/0.35 (2)	0.1083 (9)	0.2066 (8)	0.3289 (8)	0.4462 (10)
714 K	0.67/0.33 (2)	0.1069 (7)	0.2057 (6)	0.3286 (6)	0.4342 (7)
768 K	0.65/0.35 (1)	0.1072 (5)	0.2046 (4)	0.3293 (4)	0.4288 (4)
822 K	0.63/0.37 (1)	0.1071 (5)	0.2049 (4)	0.3291 (3)	0.4241 (4)
876 K	0.66/0.34 (1)	0.1068 (3)	0.2041 (3)	0.3290 (2)	0.4221 (2)
851 K	0.65/0.35 (1)	0.1072 (3)	0.2041 (3)	0.3288 (2)	0.4225 (2)
293 K	0.64/0.36 (1)	0.1063 (4)	0.2042 (3)	0.3276 (2)	0.4205 (3)

type structure (Fig. 2*a*). The space group is $Fm\bar{3}m$ (Hahn, 1995). Among three kinds of elements, Te occupied 100% of the 4(*a*) site, while Ge and Bi randomly occupied the 4(*b*) site forming an NaCl-type structure. The 4(*b*) site was not completely filled with atoms, leaving vacancies of about 20 at. % to retain the ratio of Ge + Bi:Te = 4:5. To confirm the number of vacancies, the *g* parameter of the 4(*b*) site (site-occupation rate of $Ge_{0.5}Bi_{0.5}$) was made variable. As a result, as shown in Fig. 3(*a*), *g* retained a value of 0.75–0.8 regardless of temperature. The mean volume per single atom is 31.8 Å^3 at 87 K. This metastable phase maintained its crystal structure as a single phase up to around 500 K. Above this temperature, however, the peaks of the stable phase began to appear in diffraction patterns and two phases coexisted at 550 and 605 K. The diffraction pattern obtained at 660 K indicated that the entire specimen was transformed into a stable phase. The crystal structure of this metastable $Ge_2Bi_2Te_5$ has the same atomic arrangement as the metastable $Ge_2Sb_2Te_5$ (Matsunaga *et al.*, 2004).

3.2. Crystal structure of stable phase

The structural analysis results of the $Ge_2Bi_2Te_5$ stable phase are shown in Table 2[1] and Fig. 4. The final *R* factors showed very low values that should be satisfactory, and the observed and calculated diffraction patterns closely matched. We previously examined the crystal structure of the $Ge_2Sb_2Te_5$ stable phase (Matsunaga *et al.*, 2004). The two sets of obtained results show that these two stable phases are isostructural (Fig. 2*b*). These are cubic close-packed nine-layered trigonal structures, and this $Ge_2Bi_2Te_5$ ternary alloy as well as $Ge_2Sb_2Te_5$ showed a random atomic distribution between the two kinds of atomic sites, 2:2(*d*) and 4:2(*c*). To determine the site occupancies of the Ge and Bi atoms at these two sites, we performed a Rietveld analysis while regarding $g_{Bi}^{2:2(d)}$ as an independent variable and assuming the following relationships:

[1] Supplementary data for this paper are available from the IUCr electronic archives (Reference: SO5005). Services for accessing these data are described at the back of the journal.

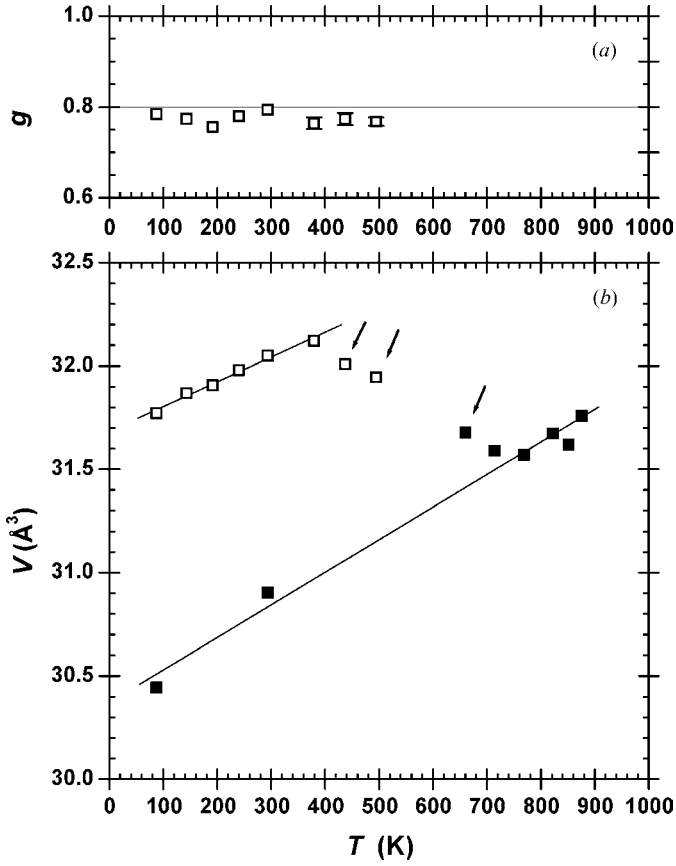

Figure 3
(*a*) Temperature dependence of the *g* parameter at the 4(*b*) site of the metastable NaCl-type structure; (*b*) temperature dependence of mean volume per single atom. Open and black filled squares show the metastable and stable phases, respectively. For data without error bars, estimated errors are smaller than the marks. The two lines in the figure were obtained by the least-squares method for each phase using the data except for those indicated by arrows.

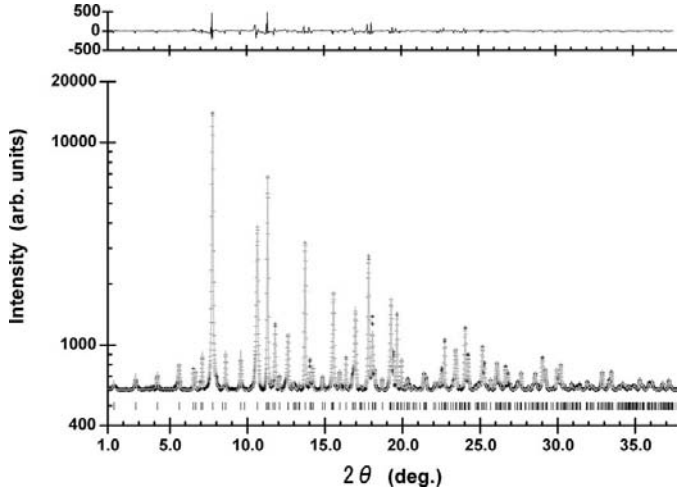

Figure 4
Observed (+) and calculated (gray line) X-ray diffraction profiles are shown for the $Ge_2Bi_2Te_5$ stable phase at 87 K. Profiles are shown in a logarithmic scale, and under them reflection markers are indicated by vertical spikes. A difference curve (observed − calculated) appears at the top of the figure in a linear scale.

Table 4
Interatomic distances (Å) in (*a*) metastable and (*b*) stable $Ge_2Bi_2Te_5$ are shown at 87 and 293 K.

			87 K	293 K
(*a*)				
Te	Ge/Bi	×6	3.0466 (2)	3.0559 (4)
(*b*)				
Te1	Ge/Bi1	×6	3.0848 (29)	3.0943 (39)
Ge/Bi1	Te2	×3	2.9779 (34)	3.0086 (46)
	Te1	×3	3.0848 (29)	3.0943 (39)
Te2	Ge/Bi1	×3	2.9779 (34)	3.0086 (46)
	Ge/Bi2	×3	3.2603 (30)	3.2801 (41)
Ge/Bi2	Te3	×3	2.9655 (26)	2.9609 (34)
	Te2	×3	3.2603 (30)	3.2801 (41)
Te3	Ge/Bi2	×3	2.9655 (26)	2.9609 (34)
	Te3	×3	3.6751 (38)	3.7128 (48)

$$g_{\rm Ge}^{2:2(d)} = 1 - g_{\rm Bi}^{2:2(d)},\ g_{\rm Bi}^{4:2(c)} = 1 - g_{\rm Bi}^{2:2(d)},\ \text{and}\ g_{\rm Ge}^{4:2(c)} = 1 - g_{\rm Bi}^{4:2(c)}, \quad (1)$$

where X and Y in g_X^Y represent the atomic species and atomic site, respectively, and g indicates the occupancy factor. To confirm the accuracy of the determined g value, we performed Rietveld analyses in which the value of $g_{\rm Bi}^{2:2(d)}$ was fixed from 0 to 1 at intervals of 0.05 or 0.1, and the other parameters were variable. The results are shown in Fig. 5. The curve in the figure is a cubic function fitted by the least-squares method; $R_{\rm wp}$ has a minimum at $g = 0.34$. The mean volume per single atom is *ca* 30.4 Å^3 at 87 K.

The metastable NaCl-type structure in the hexagonal notation is a six-layered structure in which there are infinitely alternating stacks of Te and Ge/Bi layers along the *c* axis (Fig. 2*a*). On the other hand, the stable phase has a nine-layered structure in which NaCl blocks are stacked along the *c* axis (Fig. 2*b*). An NaCl block is formed by alternately laminating Te and Ge/Bi until there are nine layers, and both the head and tail of a block always end with a Te layer. Interatomic distances are shown in Table 4 together with those for the metastable phase. In the metastable phase, each atom in the crystal has six nearest neighbors at equal distances. Also in the stable phase, the five kinds of sites hold six coordination atoms. However, in the structure of this phase, except for the Te1 atom at the 1:1(*a*) site, three shorter and three longer interatomic distances appear between the central atom and its six neighbors, which scatters interatomic distances from 2.965 to 3.675 Å (87 K). In particular, the Te—Te distance of 3.675 Å between two neighboring NaCl blocks is markedly longer than the other distances, as discovered in stable $Ge_2Sb_2Te_5$ (Matsunaga *et al.*, 2004).

3.3. Temperature dependence of crystal structure

The temperature dependences of the mean volume per single atom for both metastable and stable phases are shown in Fig. 3(*b*). The volume of the metastable phase varies almost linearly with temperature up to *ca* 400 K. The coefficient of volume expansion at room temperature is *ca* 3.8 × 10^{-5} K^{-1}. A further temperature increase led the metastable phase into a stable phase while undergoing a two-phase coexistence, and beyond 650 K the entire specimen changed into a stable phase, as mentioned above. When the measurement temperature reached 930 K, the Bragg peaks of the crystalline phase decreased abruptly and the specimen transformed into a mixed state with both a crystalline and a liquid phase. The temperature dependence of the structural parameters for the stable phase obtained by Rietveld analysis at each temperature is shown in Table 3, where g parameters were locked at constant values. The volume of the stable phase changed almost linearly with temperature, as with the metastable phase. The coefficient of volume expansion at room temperature is *ca* 5.1 × 10^{-5} K^{-1}. As seen in Fig. 3(*b*), the mean volume of the metastable phase is much larger than that of the stable phase, probably because the former contains an enormous number of vacancies in its crystal lattice. It has been revealed, however, that these vacancies play a very important role in stabilizing the metastable NaCl-type structures in the GeTe–Sb_2Te_3 pseudobinary system (Matsunaga *et al.*, 2006).

4. Discussion

4.1. Disordering between Ge and Bi atoms

In the metastable phase, Ge and Bi atoms occupied the 4(*b*) site completely at random. According to our analysis, even in the stable phase those atoms were not located at particular sites but were scattered across both 2(*c*) and 2(*d*) sites. The ratio of Ge and Bi, however, differed between sites, *i.e.* site dependency was found in the occupation rate. As shown in Table 2, the 2:2(*d*) and 4:2(*c*) sites tend to prefer Ge and Bi atoms, respectively. If the respective sites were only occupied by each favorable atom, the layer stacking of this hypothetical structure would be expressed by

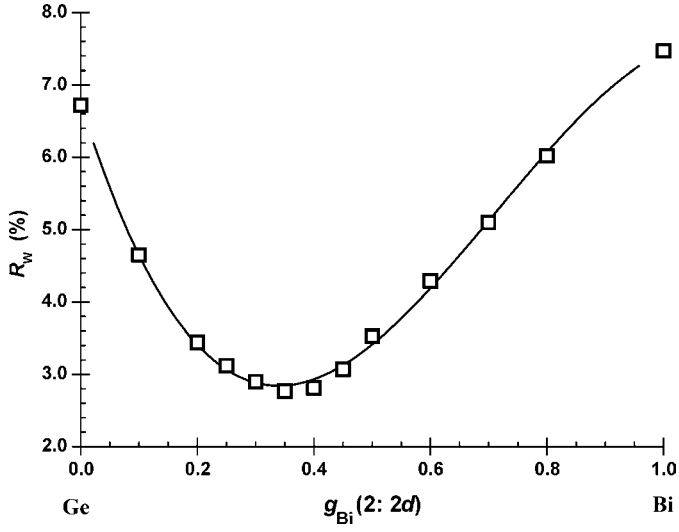

Figure 5
Agreement factor $R_{\rm wp}$ as a function of the Ge/Bi mixture ratio between 2:2(*d*) and 4:2(*c*) sites is expressed for refinements with fixed values of parameter g at the 2:2(*d*) site at intervals of 0.05 or 0.1 from 0.0 to 1.0.

Table 5
Structural parameters for $Ge_{1.5}Bi_{2.5}Te_5$ as shown by Karpinsky *et al.* (1998*a*).

The atom notation for each site follows Karpinsky *et al.*'s description in this table. Parameter μ indicates the occupation factors in atomic parts. The last column shows the parameters (atomic positions) obtained by Rietveld refinement performed with our $Ge_2Bi_2Te_5$ diffraction data assuming Karpinsky *et al.*'s occupation factors (μs) at each site. Final *R* factors for this analysis were $R_{wp} = 0.0316$, $R_p = 0.0199$, $R_I = 0.0158$, and R_{wp} expected = 0.0376. These R_{wp} and R_I values are, however, as expected, slightly inferior to those shown in Table 1.

	Site	μ	*x*	*y*	*z*	*z*
Te5	1:1(*a*)	0.79Te + 0.21Bi	0	0	0	0
Me2	2:2(*d*)	0.54Ge + 0.46Bi	2/3	1/3	0.1042 (3)	0.1088 (3)
Te4	3:2(*d*)	0.94Te + 0.06Bi	1/3	2/3	0.2035 (3)	0.2041 (2)
Me1	4:2(*c*)	0.63Bi + 0.17Ge + 0.20Te	0	0	0.3284 (2)	0.3266 (2)
Te3	5:2(*d*)	0.96Te + 0.04Ge	2/3	1/3	0.4221 (4)	0.4210 (2)

$$[C] : \frac{\text{Te}}{a} \cdot \frac{\text{Ge}}{b} \cdot \frac{\text{Te}}{c} \cdot \frac{\text{Bi}}{a} \cdot \frac{\text{Te}}{b} \cdot \frac{\text{Te}}{c} \cdot \frac{\text{Bi}}{a} \cdot \frac{\text{Te}}{b} \cdot \frac{\text{Ge}}{c} \cdot \frac{\text{Te}}{a}.$$

Note that this atomic configuration retains the composition of $Ge_2Bi_2Te_5$. On the other hand, if this compound had a totally opposite atomic configuration in the 2:2(*d*) and 4:2(*c*) sites to the [*C*] model, its layer staking would be shown as

$$[R] : \frac{\text{Te}}{a} \cdot \frac{\text{Bi}}{b} \cdot \frac{\text{Te}}{c} \cdot \frac{\text{Ge}}{a} \cdot \frac{\text{Te}}{b} \cdot \frac{\text{Te}}{c} \cdot \frac{\text{Ge}}{a} \cdot \frac{\text{Te}}{b} \cdot \frac{\text{Bi}}{c} \cdot \frac{\text{Te}}{a}.$$

In the Ge_2'Sb'$_2Te_5$ case, these two perfect-order [*C*] and [*R*] models correspond to the structural models of Kooi & De Hosson (2002) and Petrov *et al.* (1968), respectively. However, these four perfect-order models gave unsatisfactory Rietveld refinements (Fig. 5 in this paper and Fig. 4 in our previous paper; Matsunaga *et al.*, 2004). In the actual compounds, Ge and Bi(Sb) were actually scattered across both 2:2(*d*) and 4:2(*c*) sites. The ratio of Ge to Bi(Sb), however, differed between the sites; Ge atoms prefer the 2:2(*d*) site, while Bi(Sb) atoms tend to select the 4:2(*c*) site, as mentioned above.

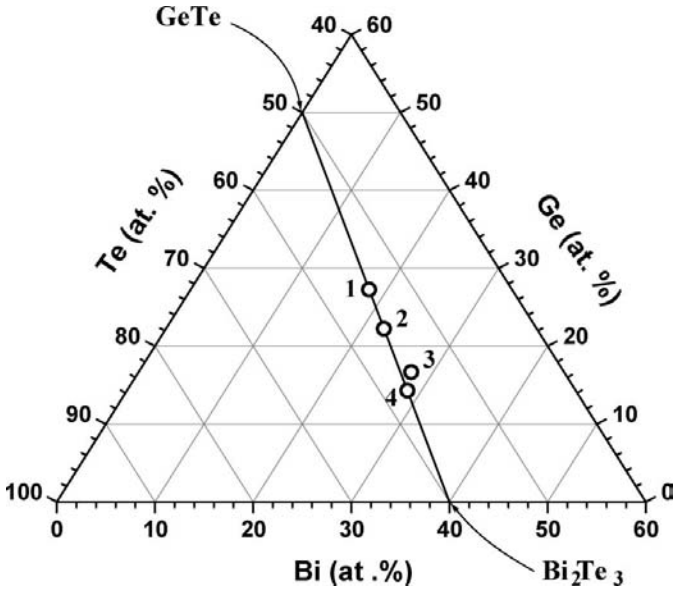

Figure 6
In this diagram of the Ge–Bi–Te ternary system, the GeTe–Bi_2Te_3 pseudobinary system is indicated by the line. The compositions of intermetallic compounds (1) $Ge_3Bi_2Te_6$, (2) $Ge_2Bi_2Te_5$, (3) $Ge_{1.5}Bi_{2.5}Te_5$ and (4) $GeBi_2Te_4$ are shown by open circles in the diagram.

4.2. Comparison with neighboring homologous structures

As mentioned in §1, Karpinsky *et al.* (1998*a*) analyzed the crystal structure of $Ge_{1.5}Bi_{2.5}Te_5$ by a single-crystal X-ray diffraction method, showing that this compound has a stable $Ge_2Sb_2Te_5$ nine-layered trigonal isostructure. In the GeTe–Bi_2Te_3 pseudobinary system, intermetallic compounds (1) $Ge_3Bi_2Te_6$ (33-layer structure) and (4) $GeBi_2Te_4$ (21-layer structure) have already been found near (2) $Ge_2Bi_2Te_5$ and (3) $Ge_{1.5}Bi_{2.5}Te_5$ (Fig. 6). Based on their analyses, partial atomic disordering at all five kinds of atomic sites has been observed, even at the three Te sites in the $Ge_{1.5}Bi_{2.5}Te_5$ compound (Table 5). As shown in Fig. 6, however, this compound's composition is situated very close to $GeBi_2Te_4$, apart from the ideal composition of the nine-layer structure, $Ge_2Bi_2Te_5$, which is at the off-stoichiometric point from the GeTe–Bi_2Te_3 pseudobinary line. This would cause atomic disordering throughout the five atomic sites. However, even $Ge_2Bi_2Te_5$, including its metastable phase, may have a small amount of partial disordering over more than two atomic sites, as seen in $Ge_{1.5}Bi_{2.5}Te_5$. This situation calls for further precise examinations, such as those using neutron diffraction and/or single-crystal X-ray diffraction methods.

5. Conclusion

$Ge_2Bi_2Te_5$ in the GeTe–Bi_2Te_3 pseudobinary system has two crystalline phases, metastable and stable, as does $Ge_2Sb_2Te_5$ in the GeTe–Sb_2Te_3 system. Each phase is isostructural with a corresponding $Ge_2Sb_2Te_5$ phase. The metastable phase crystallizes into a six-layered cubic close-packed (NaCl-type) structure in which Ge/Bi and Te layers are piled alternately. The Ge/Bi layer in the metastable phase contains as much as 20 at. % vacancies, which make the mean volume per single atom larger than that in the stable phase. On the other hand, in the stable phase, Te and Ge/Bi are stacked alternately nine times to form an NaCl block, and then the blocks are piled to construct a nine-layered trigonal structure with cubic close-packed stacking. Both ends of the NaCl block are covered with Te layers.

Synchrotron radiation experiments were performed on the BL02B2 beamline at SPring-8 with the approval of the Japan Synchrotron Radiation Research Institute (JASRI). We express our sincere gratitude to Drs K. Kato and K. Osaka at JASRI and to graduate students N. Yasukawa, A. Yoshimura and T. Murata at the Graduate School of Science of Osaka Prefecture University for their assistance in the experiment.

References

Hahn, T. (1995). *International Tables for Crystallography*, Vol. A. Dordrecht: Kluwer Academic Publishers.

Izumi, F. & Ikeda, T. (2000). *Mater. Sci. Forum*, **321–324**, 198–203.
Karpinsky, O. G., Shelimova, L. E., Kretova, M. A. & Fleurial, J.-P. (1998*a*). *J. Alloys Compd.* **265**, 170–175.
Karpinsky, O. G., Shelimova, L. E., Kretova, M. A. & Fleurial, J.-P. (1998*b*). *J. Alloys Compd.* **268**, 112–117.
Kooi, B. J. & De Hosson, J. Th. M. (2002). *J. Appl. Phys.* **92**, 3584–3590.
Matsunaga, T., Kojima, R., Yamada, N., Kifune, K., Kubota, Y., Tabata, Y. & Takata, M. (2006). *Inorg. Chem.* **45**, 2235–2241.
Matsunaga, T., Yamada, N. & Kubota, Y. (2004). *Acta Cryst.* B**60**, 685–691.
Nishibori, E., Takata, M., Kato, K., Sakata, M., Kubota, Y., Aoyagi, S., Kuroiwa, Y., Yamakata, M. & Ikeda, N. (2001). *Nucl. Instrum. Methods A*, **467–468**, 1045–1048.
Petrov, I. I., Imamov, R. M. & Pinsker Z. G. (1968). *Sov. Phys. Crystallogr.* **13**, 339–342.
Rietveld, H. M. (1969). *J. Appl. Cryst.* **2**, 65–71.
Shelimova, L. E., Karpinskii, O. G., Konstantinov, P. P., Avilov, E. S., Kretova, M. A. & Zemskov, V. S. (2004). *Inorg. Mater.* **40**, 451–460.
Yamada, N., Ohno, E., Nishiuchi, K., Akahira, N. & Takao, M. (1991). *J. Appl. Phys.* **69**, 2849–2856.
Yusu, K., Ashida, S., Naomasa, N., Oomachi, N., Morishita, N., Ogawa, A. & Ichihara, K. (2002). *Technical Digest of ISOM/ODS*, pp. 413–414.